

# Thermodynamic, kinetic, and magnetic properties of a $\text{Ni}_{54}\text{Fe}_{19}\text{Ga}_{27}$ magnetic shape-memory single crystal

O. Heczko,<sup>1</sup> S. Fähler,<sup>1</sup> T. M. Vasilchikova,<sup>2</sup> T. N. Voloshok,<sup>2</sup> K. V. Klimov,<sup>2</sup> Yu. I. Chumlyakov,<sup>3</sup> and A. N. Vasiliev<sup>2</sup>

<sup>1</sup>*IFW Dresden, Institute for Metallic Materials, P.O. Box 27 01 16, 01171 Dresden, Germany*

<sup>2</sup>*Moscow State University, Moscow, 119991, Russia*

<sup>3</sup>*Tomsk State University, Tomsk, 634050, Russia*

(Received 21 December 2007; revised manuscript received 13 March 2008; published 2 May 2008)

Ferromagnetic Heusler alloys exhibiting martensitic transformations are known to change their shape in an external magnetic field. Magnetization, electric resistance, and specific heat as a function of temperature are examined in  $\text{Ni}_{54}\text{Fe}_{19}\text{Ga}_{27}$  single crystal. Structural transition appears as sharp anomaly in these dependencies. This points to an avalanchelike character of martensitic transformation. The jump in resistivity at the structural phase transition and the lower density of states at the Fermi level in the martensite phase supports the hypothesis of the Jahn-Teller origin of the martensitic transformation. Magnetic measurements show that transformation to the martensitic phase is accompanied by the increase of spontaneous magnetization and an increase of magnetocrystalline anisotropy. Magnetization increase is due to different Curie temperatures of austenite and martensite. These were determined from critical behavior using Arrott plot. Additional analysis of magnetic behavior indicates ferrimagnetic ordering in this nonstoichiometric compound. Intrinsic properties of the compound are analyzed with respect to both of the actuation modes possible in magnetic shape-memory alloys. However, neither a magnetically induced martensite transformation nor a magnetically induced reorientation of variants has been observed.

DOI: [10.1103/PhysRevB.77.174402](https://doi.org/10.1103/PhysRevB.77.174402)

PACS number(s): 75.50.Cc, 65.40.Ba, 75.30.Gw, 75.80.+q

## INTRODUCTION

Intermetallic compounds with a shape-memory effect driven by a magnetic field are intensively studied since they offer unique opportunities to obtain large reversible deformations without temperature variations.<sup>1</sup> This effect is observed in ferromagnets exhibiting martensitic transformations. Martensite transformation is a structural phase transition from high temperature, high symmetric austenite phase to a low temperature, low symmetry martensite phase. This phase transition is diffusionless, as the mutual rearrangement or relative displacements of atoms are small compared to interatomic distances. When austenite and martensite phases exhibit different magnetizations, an external magnetic field can be used to stabilize the phase exhibiting the higher moment. Typically the martensite phase exhibits higher moments. Thus, in the vicinity of the transition temperature, a magnetic field at constant temperature can be used for the formation of magnetically induced martensite (MIM).

Martensite phases are characterized by the high mobility of microstructural twin boundaries which may result in rubberlike behavior. This allows the use of a second mechanism for shape changes at constant temperature below the martensitic transformation temperature. The shape change occurs by rearrangement of martensitic variants in a magnetic field. This magnetically induced rearrangement (MIR) is possible in alloys where the magnetocrystalline anisotropy energy exceeds the energy necessary to move the twin boundaries. In this case, the reduction of the total energy of a ferromagnet in a magnetic field takes place through the increase of the volume of the variants whose magnetization easy axis is close to the direction of the external magnetic.<sup>2-4</sup> The reduction is not via rotation of magnetization vectors in magnetic domains.

These two shape-memory effects driven by magnetic fields are observed in the Heusler alloys close to stoichiometric  $\text{Ni}_2\text{MnGa}$ ,<sup>5-7</sup> as well as in the binary alloys Fe-Pd (Ref. 8) and Fe-Pt.<sup>9</sup> Structural and magnetic phase transitions in Heusler alloys were found to be very sensitive to deviations from stoichiometry. This opens the possibility of deliberate variations of the transition temperatures up to their coincidence. This coupling is of benefit when inducing phase transformations by a magnetic field.<sup>10</sup> Under merged magnetic and structural phase transitions, it is possible to transform samples from paramagnetic austenite state to ferromagnetic martensite state under action of a magnetic field.

Applications of intermetallics with magnetically driven shape memory are hampered by the brittleness of these ordered alloys. Thus, new compounds are desirable. Less brittle and partly ductile intermetallic compounds of  $\text{Ni}_{2+x+y}\text{Fe}_{1-x}\text{Ga}_{1-y}$  were proposed<sup>13</sup> in addition to  $\text{Ni}_2\text{MnAl}$  (Ref. 11) and  $\text{Co}_2\text{NiGa}$  (Ref. 12) alloys. Temperatures of structural and magnetic phase transitions strongly vary with deviations from stoichiometry in  $\text{Ni}_{2+x+y}\text{Fe}_{1-x}\text{Ga}_{1-y}$  alloys.

The stoichiometric Heusler alloy  $\text{Ni}_2\text{FeGa}$  can be obtained only as a thin ribbon by rapid quenching from the melt<sup>14</sup> without segregation of secondary phases. The formation of completely or partially ordered  $\beta$ -phase is in competition with the formation of the disordered  $\text{A1}$   $\gamma$ -phase when using equilibrium methods of synthesis and thermal treatment. A fully ordered phase of a Heusler alloy  $X_2YZ$  with  $L2_1$  structure can be derived from a body-centered cubic cell, where  $X$  atoms are situated at its corners and  $Y$  and  $Z$  atoms alternate in the cubic centers. At the martensitic transformation temperature  $T_M \sim 150$  K, a stoichiometric  $\text{Ni}_2\text{FeGa}$  Heusler alloy transforms from the cubic  $L2_1$  into the tetragonal  $L1_0$  structure.

In compounds with only partial atomic order in austenite phase and in compositions away from stoichiometry, the

martensite transition can occur via intermediate modulated  $10M$  and  $14M$  phases.<sup>15</sup> At stoichiometric composition, the Curie temperature in Heusler alloy  $\text{Ni}_2\text{FeGa}$  is relatively high,  $T_C \sim 430$  K. Similar to other Heusler alloys, magnetism in these compounds is associated mainly with  $Y$  atoms. Both calculations of band structure and experimental studies show that the saturation magnetization in the martensite phase ( $\mu_{\text{sat}} = 3.170\mu_B$ ) exceeds calculated saturation magnetization in the austenite phase ( $\mu_{\text{sat}} = 3.035\mu_B$ ).<sup>16</sup> By lowering the Fe content and increasing the Ni content, the temperature of martensitic transformation increases and the Curie temperature decreases.

Earlier, the physical properties of  $\text{Ni}_{2+x+y}\text{Fe}_{1-x}\text{Ga}_{1-y}$  alloys were investigated in polycrystalline samples obtained by arc melting or in the form of rapid quenched ribbon.<sup>16</sup> Phase transitions in these alloys are usually seen as smeared anomalies. The fundamental thermodynamic and magnetic properties of  $\text{Ni}_{54}\text{Fe}_{19}\text{Ga}_{27}$  single crystal are investigated here in order to examine whether this is an intrinsic feature of the crystalline structure or an extrinsic feature depending on microstructure. Phase transformations of  $\text{Ni}_{54}\text{Fe}_{19}\text{Ga}_{27}$  single crystal are analyzed by electrical resistance, specific heat, and magnetization measurements as a function of temperature. Suitability of the material for both actuation mechanisms (MIM and MIR) is discussed.

### EXPERIMENT

Single crystals with a nominal composition  $\text{Ni}_{54}\text{Fe}_{19}\text{Ga}_{27}$  were grown by the Bridgeman method from the melt.<sup>15</sup> During the process of crystal growth, the chemical composition of the ingot changed resulting in variations of phase transition temperatures between samples cut from the different parts of the ingot. Energy dispersive spectroscopy analysis of the sample used for magnetization measurements showed a composition of  $\text{Ni}_{53.7}\text{Fe}_{20.2}\text{Ga}_{26.1}$  with deviation less than 0.5 at. % All samples used for measurements of physical properties were cut from adjacent locations of the ingot in order to minimize influence by the composition gradient. The as-grown single crystal was slowly cooled without additional heat treatment.

The lattice constant of cubic austenite phase  $a = 0.575$  nm at room temperature was determined by x-ray diffraction measurement from (220) and (440) reflections. The presence of very low intensity superstructure (111) reflection suggests a high degree of  $L2_1$  ordering in austenite at room temperature. An existence of long range order was also confirmed by transmission electron microscopy studies on as-grown crystal. Observed existence of  $L2_1$  order agrees with the neutron diffraction studies of  $\text{Ni}_{54}\text{Fe}_{19}\text{Ga}_{27}$  alloy.<sup>16</sup> However, the order in the studied alloy can only be partial due to the deviation from stoichiometry.

Temperature dependence of the resistance  $\rho$  of the single crystal from 77 to 300 K was measured by the four-point contact method. Rectangular sample had the dimensions if  $1 \times 1 \times 8$  mm<sup>3</sup>. Temperature dependence of the specific heat  $C$  in the range of 5–300 K was measured by the relaxation method in “Termis” calorimeter and in the range of 2–20 K by “Quantum Design” physical property measurement system.

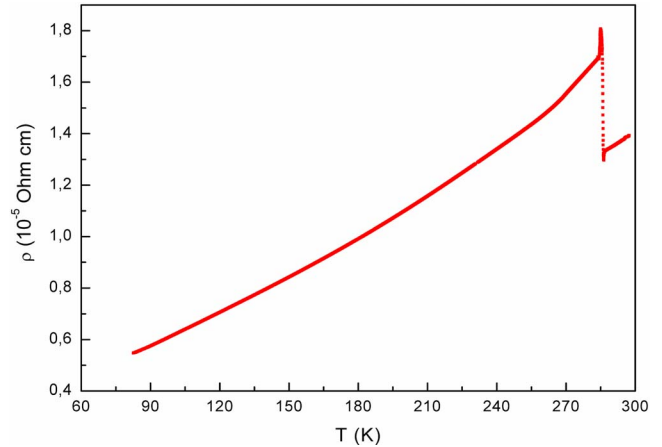


FIG. 1. (Color online) Temperature dependence of resistivity  $\rho$  during heating.

Temperature and field dependent magnetic properties were studied by Quantum Design physical property measurement system using a vibrating sample magnetometer insert. Heating and cooling rates were 5 deg/min. The rectangular sample had approximate dimensions of  $3.5 \times 3.7 \times 3.8$  mm<sup>3</sup>. Hysteresis curves have been corrected for demagnetization effects, i.e., the shear of the curves was eliminated using a demagnetizing factor  $N$  determined from the austenite phase with low magnetic anisotropy.

### RESULTS AND DISCUSSION

Figure 1 shows the temperature dependence of resistance  $\rho$  measured at increasing temperature. In the range from 77 to 285 K, the resistance approximately increased three times but it does not exhibit any features that would suggest an intermartensitic transition. At  $T_M = 285$  K, a sharp drop is seen in the  $\rho$  vs  $T$  curve, which corresponds to the transition from martensite to austenite phase. The change of resistance at martensite/austenite phase transition can be ascribed to the variation of the electron phase density of states at the Fermi level. Calculations of the band structure of cubic (austenite)  $\text{Ni}_2\text{FeGa}$  show a peak in the density of states near the Fermi level. This peak is associated with the  $3d$  electrons of Ni and splits at the phase transition resulting in an increase of the resistivity. Therefore, the driving force for martensitic transformation can be the band Jahn-Teller effect.<sup>16</sup> An additional contribution to the increase of resistance at transition to low temperature phase can be due to the decrease of the carriers' mobility as the carriers are scattered at martensite twin boundaries.

The specific heat  $C$  vs  $T$  dependence for  $\text{Ni}_{54}\text{Fe}_{19}\text{Ga}_{27}$  single crystal is shown in Fig. 2 in logarithmic scale. A very sharp peak corresponding to first order phase transition is apparent at  $T_M = 288$  K. The amplitude and narrowness of the anomaly at the structural phase transition suggest an avalanche-like character of martensitic transformation, which is not hindered by grain boundaries. Another weak anomaly is present at temperature at  $T_C = 291$  K. This might suggest an additional structural transformation or magnetic phase tran-

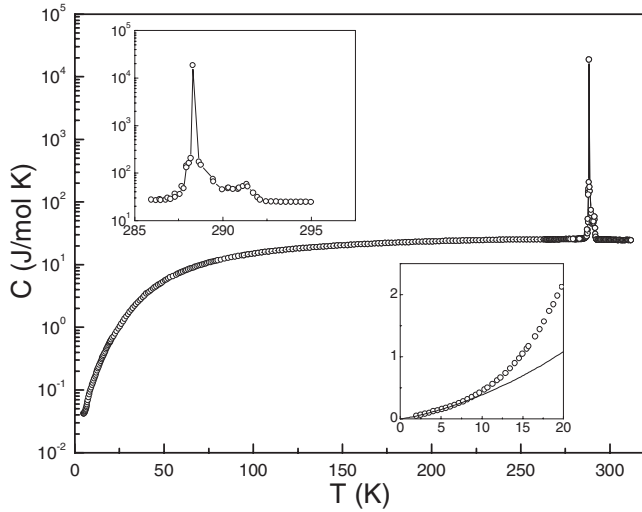


FIG. 2. Temperature dependence of specific heat  $C$  of the  $\text{Ni}_{54}\text{Fe}_{19}\text{Ga}_{27}$  single crystal during heating. Upper inset: enlarged portion of  $C$  vs  $T$  curve in vicinity of structural phase transition; lower inset: the experimental data (circles) and fit by Eq. (1) (solid line) of the low temperature specific heat.

sition. However, no discernible changes of low or high field magnetization curves are observed in this region (Fig. 3), thus excluding magnetic phase transition.

The behavior of specific heat at low temperatures is given by the formula

$$C = \gamma T + \alpha T^{3/2} + \beta T^3, \quad (1)$$

where the first term represents electronic contribution, the second term represents contribution by magnetic excitations, and the third term corresponds to the phonon contribution.

The electronic contribution to specific heat is characterized by Sommerfeld coefficient  $\gamma$ , which is proportional to density of states at the Fermi level:

$$\gamma = (2/3)\pi^2 k_B^2 N(\epsilon_F). \quad (2)$$

The experimental value  $\gamma = 14 \text{ mJ/mol K}^2$  corresponds to a density of electronic states  $N(\epsilon_F) \sim 6 \times 10^{22} \text{ cm}^{-3} \text{ eV}^{-1}$ . This value is in qualitative agreement with the band structure calculations.<sup>15</sup> The second term in specific heat can be fitted with a coefficient  $\alpha \sim 7 \times 10^{-3} \text{ J/mol K}^{3/2}$ . This coefficient is determined by several unknown parameters of the magnetic subsystem in ferromagnetic  $\text{Ni}_{54}\text{Fe}_{19}\text{Ga}_{27}$  among which are the rigidity of longitudinal spin waves and the gap due to the magnetocrystalline anisotropy.<sup>18</sup>

Phonons contribution with coefficient,

$$\beta = \pi^4 R n \Theta^{-3}, \quad (3)$$

where  $R$  is the gas constant and  $n$  is number of atoms per formula unit, allows determination of the Debye temperature. This value was estimated as  $\Theta = 290 \text{ K}$  in the sample studied.

Temperature dependencies of magnetization measured at different applied fields of a  $\text{Ni}_{54}\text{Fe}_{19}\text{Ga}_{27}$  single crystal over a temperature range of 10–400 K are summarized in Fig. 3(a). The region around room temperature is enlarged in Fig. 3(b). Temperatures of structural and magnetic transformations

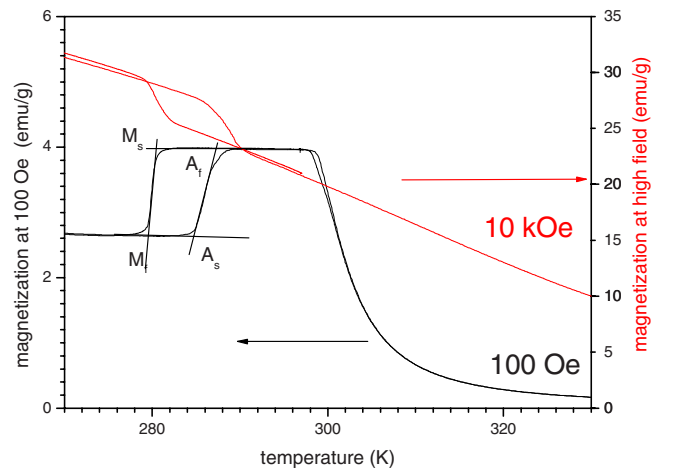
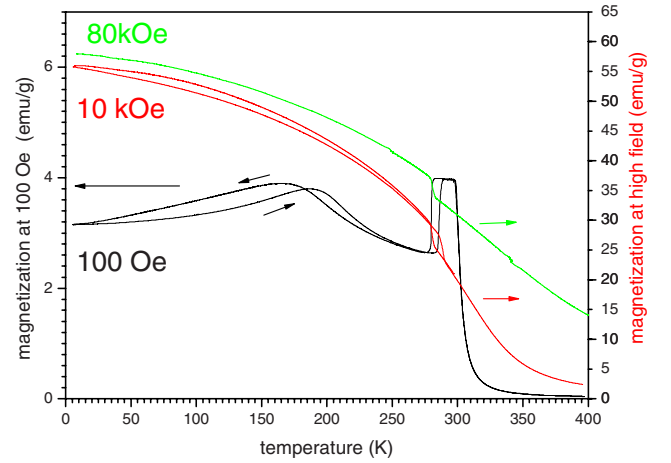


FIG. 3. (Color online) Temperature dependence of magnetization in 100 Oe, 10 kOe, and 80 kOe applied fields of the  $\text{Ni}_{54}\text{Fe}_{19}\text{Ga}_{27}$  single crystal. (a) The complete temperature range from 10 to 400 K. (b) enlarged area around the transition temperatures. The lines indicate how the transition temperatures have been extracted from the measurement in 100 Oe.

were determined from measurement of low field magnetization or dc susceptibility  $\chi$ , at 10, 20, and 100 Oe in the range of 10–400 K. The curves have the same shapes and they are close to each other and for the sake of clarity only a curve measured at 100 Oe is shown. From measurements above room temperature, the ferromagnetic Curie temperature of the austenite can be estimated at  $T_C = 305 \text{ K}$ . However, a large ferromagnetic tail does not allow an accurate determination by this simple approach. Although this is the usual way to determine  $T_C$  in magnetic shape-memory alloys, the determination is somehow arbitrary. Using functional dependence of reciprocal susceptibility above  $T_C$ ,  $1/\chi \approx (T - T_C)$ , the paramagnetic Curie point was determined to be 300 K, as shown in Fig. 4. The reciprocal susceptibility is, however, not linear as expected for ferromagnetic materials. The convex shape well above the Curie point suggests possible ferromagnetic or noncollinear ordering in the crystal.<sup>19</sup>

The martensite phase with low symmetry exhibits a higher magnetocrystalline anisotropy compared to the highly

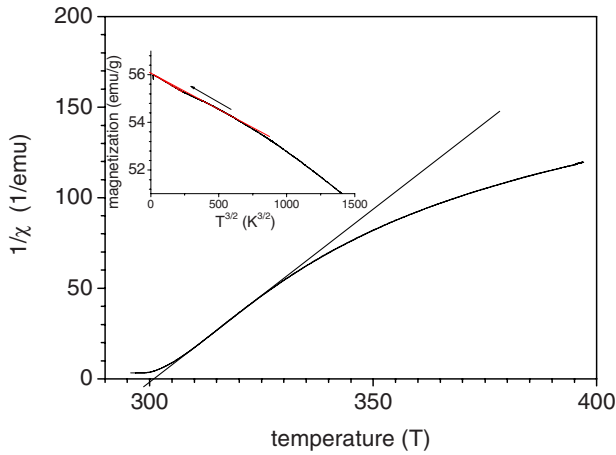


FIG. 4. (Color online) Reciprocal susceptibility at 10 Oe in paramagnetic region. The convex shape deviation from linearity suggests ferrimagnetic ordering. Inset: fit of the low temperature region of magnetization using spin-wave theory.

symmetric austenite. This makes it more difficult to magnetize a multivariant martensite sample. Thus, low field magnetization (or susceptibility) decreases upon transformation and therefore allowing a precise determination of martensitic transformation. The sketched linear intersections in Fig. 3(b) give for a direct transformation a martensite start temperature of  $M_s=280$  K and a martensite finish temperature of  $M_f=279$  K. For the reverse transformation during heating, the austenite start temperature is  $A_s=285$  K and austenite finish temperature is  $A_f=288$  K. Evidently, the structural transition is quite sharp with a hysteresis  $\Delta T \sim 6$  K between the direct and reverse transformations. The temperatures of transformation and the sharpness of the transformation agree well with the values determined from the measurements of the resistivity and specific heat.

However, in contrast to resistivity and specific heat, susceptibility shows additional features at low temperatures, which is also not apparent in magnetization measurements in applied fields of 10 or 80 kOe. Below the initial decrease due to the martensite transformation, further cooling results in an increase of susceptibility and a broad peak at about 170 K can be observed. During heating, a hysteresis occurs and the peak shifts to around 190 K. The observed changes may indicate the existence of a weak intermartensitic transition in this region, in which some spin rearrangement occurs. However, the absence of observed anomalies in resistivity and specific heat measurements suggests that purely magnetic transition, e.g., a ferrimagnetic compensation point should also be considered.

Also shown in Fig. 3 are magnetization measurements in applied fields of 10 and 80 kOe. As demonstrated later, these fields are significantly above the anisotropy field. Hence, the curve represents the behavior of the saturation magnetization. Saturation magnetization increases by about 10% at the martensite transformation. In general, the increase agrees with the calculations showing that the total moment increases upon transformation to martensite.<sup>16</sup> However, the measured increase is much larger than the increase calculated for the stoichiometry compound. Moreover, no significant

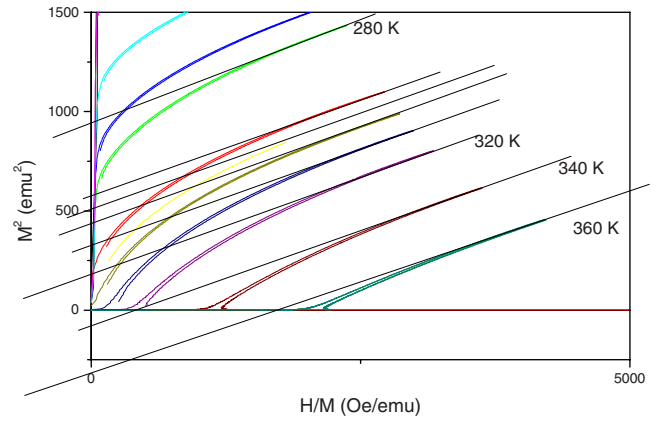


FIG. 5. (Color online) Arrott curves  $M^2$  vs  $H/M$  and linear extrapolation to obtain the spontaneous magnetization  $M_s$ . Only selected curves are shown for clarity.

increase of the saturation magnetization was experimentally observed for the stoichiometric compound.<sup>16</sup> These differences may be due to the differences in magnetic ordering (ferri- or ferromagnetic) and/or due to different Curie temperatures of martensite and austenite phases.

The method suggested by Arrott was used,<sup>20,21</sup> employing molecular field theory to determine the ferromagnetic Curie temperature. The magnetization curves of martensite and austenite phases were measured up to maximum field of 90 kOe at different temperatures close to transition. From the functional dependence of magnetization  $M^2$  vs  $H/M$ , the square of spontaneous magnetization (at zero field)  $M_s^2$  was determined by extrapolation, as shown in Fig. 5. The Curie temperature of the austenite is then determined from the linear extrapolation of  $M_s^2$  vs  $T$  to zero magnetization, as shown in Fig. 6. This gives a ferromagnetic Curie temperature of austenite  $T_c^A=331$  K, which is larger than  $T_c$  determined from the susceptibility. Determined Curie temperature is about 100 K lower than for the stoichiometry compound.<sup>16</sup>

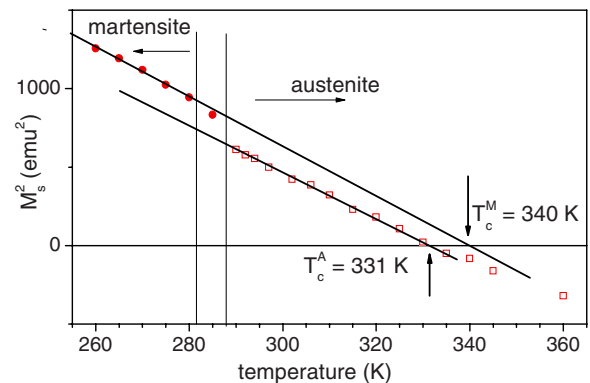


FIG. 6. (Color online) Arrott plot of spontaneous magnetization  $M_s^2$  vs temperature to determine ferromagnetic Curie temperatures of austenite and martensite. The spontaneous magnetization was obtained by extrapolation, as shown in Fig. 5. Ferromagnetic Curie points of austenite and martensite phases were determined by extrapolation to zero magnetization. Vertical lines mark the onset and completion of the martensite transformation. In interval between the lines, the compounds is in a mixed state.

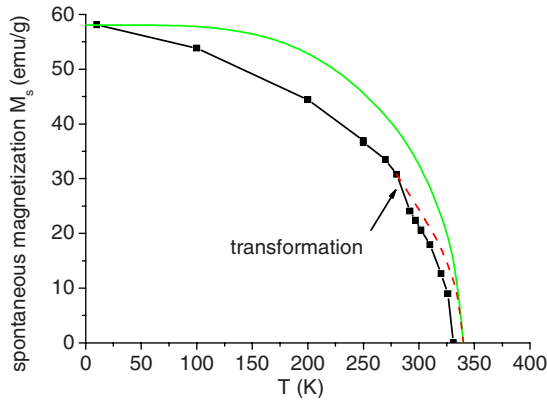


FIG. 7. (Color online) Temperature dependence of spontaneous magnetization of Ni-Fe-Ga and comparison with the theoretical curve for  $J=\frac{1}{2}$  scaled for the Curie temperature and spontaneous magnetization of martensite. The dotted line is an extrapolated curve of martensite above transformation.

This method can also be used to extract the Curie temperature of the martensite. By extrapolation of the linear fit of spontaneous magnetization of martensite close to transition temperature, we obtain an approximation for the Curie temperature of the martensite, which is about  $T_C^M=340$  K. Although this fit is more tentative, it allows at least an estimation of the  $T_C^M$  of ferromagnetic martensite, which is not otherwise accessible. It has been recently discussed that molecular field theory overestimated the Curie temperature.<sup>22</sup> Using the equation of state and proper critical exponents<sup>21</sup> and the procedure described above, we obtain Curie temperatures of austenite and martensite  $T_C^A=310$  K and  $T_C^M=317$  K, respectively. Despite this variation, the important feature is the difference between the Curie temperatures of the austenite and the martensite regardless of the method used. This difference explains the increase of the saturation or spontaneous magnetization during martensite transformation.

The magnetization extracted from the Arrott analysis has been used to plot the temperature dependent spontaneous magnetization (Fig. 7). The Brillouin function for  $J=1/2$  scaled to  $T_C^M$  is plotted for comparison. This is usually an appropriate description for 3d metals with quenched orbital moments. The measured data obviously exhibit a different shape, which is more typical for ferrimagnetic order.

At a low temperature range,  $T < 70$  K, the saturation magnetization at 80 kOe fits the relation derived from spin-wave theory,

$$M(T) = M(0)(1 - AT^{3/2}), \quad (4)$$

which gives a magnetization at 0 K of  $M(0)=56.05$  emu/g. This yields a magnetic moment per formula unit of  $2.44\mu_B$  for determined composition  $\text{Ni}_{53.7}\text{Fe}_{20.2}\text{Ga}_{26.1}$ . This value is lower than the value  $3.17\mu_B$  experimentally measured for the stoichiometric compound<sup>16</sup> and higher than the magnetic moment,  $2.4\mu_B$  of  $\text{Ni}_{54}\text{Fe}_{19.3}\text{Ga}_{26.5}$  alloy.<sup>23</sup> Although only three data points are available, one can use them to analyze the influence of Fe content on total magnetic moment. A linear extrapolation gives about 4 at. % Fe concentration for

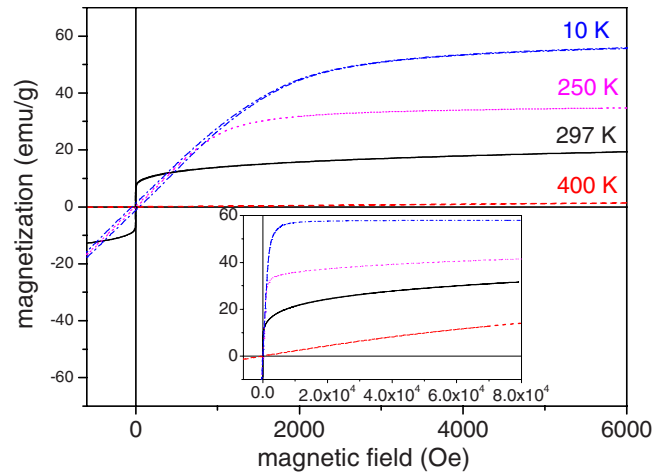


FIG. 8. (Color online) Magnetization loops in a  $\text{Ni}_{54}\text{Fe}_{19}\text{Ga}_{27}$  single crystal in a paramagnetic austenite state (400 K), ferromagnetic austenite state (297 K), and ferromagnetic martensite state (250 and 10 K). The inset shows the first quadrant of the same loops in the high field range.

zero magnetic moment. Although the extrapolation may suffer from a large error, this suggests that the main contribution to the magnetic moment originated from Fe atoms, i.e., on Y atom in  $X_2YZ$  formula, as it is usual for Heusler alloys, particularly for  $\text{Ni}_2\text{MnGa}$ .<sup>24,25</sup> This is also supported by neutron diffraction measurement.<sup>17</sup> In the nonstoichiometric compound examined here, the positions not occupied by Fe are expected to be mostly filled by Ni. In a simplified local picture, however, it is not clear if the Ni moments are coupled parallel or antiparallel to the Fe moments.

The spin-wave stiffness coefficient  $D$  from the spin dispersion law  $\hbar\omega=Dq^2$  can be calculated using the coefficient  $A=5.27 \times 10^{-5}$  from Eq. (4). This gives  $D=128$  meV  $\text{\AA}^2$ , which is larger than for stoichiometric compound.<sup>16</sup>

There is no discernible shift of martensite transformation temperatures when applying 10 kOe or even 80 kOe compared to the low field measurement, as shown in detail in Fig. 3(b). This is despite the relatively large change of the saturation magnetization. Thus, one can conclude that the magnetic field does not significantly influence the structural transition. High magnetic field does, however, result in a significantly increased magnetization within the complete temperature range compared to 10 kOe. This is expected at higher temperatures as the external field adds up the molecular field, an effect called forced magnetization. This, however, should not be the case for the temperatures approaching 0 K, where thermal fluctuations should vanish. This observation, however, could be explained by an existence of ferrimagnetic order where a strong field can partially align both antiparallel coupled sublattices in the direction of the applied field.

Figure 8 shows the magnetization loops at selected temperatures including measurements in a paramagnetic austenite state (400 K), a ferromagnetic austenite state (297 K), and a ferromagnetic martensite state (250 K and 10 K). The inset shows the first quadrant of the high field range. A nearly linear line with low curvature is observed at 400 K, as

expected for the paramagnetic state. In the ferromagnetic state, the hysteresis loops in austenite and martensite states are very similar. The coercive force of austenite was estimated as  $H_C=3$  Oe. At a transition to martensite state, the coercive force increases to  $H_C=8$  Oe and it reaches  $H_C=40$  Oe at 10 K. The larger tilt of the curves measured at a martensite state points to uniaxial magnetocrystalline anisotropy of martensite. The demagnetization factor determined from the magnetization curve of austenite can be used to deshear the  $M$  vs  $H$  curves if one assumes that the anisotropy field of the austenite phase is negligible. This allows estimation of the magnetocrystalline anisotropy of  $\text{Ni}_{54}\text{Fe}_{19}\text{Ga}_{27}$  martensite from the anisotropy field.<sup>26</sup> The anisotropy constants are  $0.5 \times 10^5$  J/m<sup>3</sup> at 10 K and  $0.17 \times 10^5$  J/m<sup>3</sup> at 250 K. The given values can be only considered as a rough estimate since the distribution of martensite variants is not known. Usually, the mixture of variants with hard and easy axes of magnetization leads to an underestimate of magnetocrystalline anisotropy. The observed value at 10 K is about half of the magnitude reported for the stoichiometric compound<sup>16</sup> and about six times less than for Ni-Mn-Ga compound exhibiting magnetic shape memory effect.<sup>26</sup>

The magnetization curves of martensite resulting from cooling in 0 and 80 kOe over transformation were measured in order to evaluate the effect of the magnetic field on the martensite variant distribution or martensite microstructure. The difference between these curves was very slight. This suggests that the effect of the magnetic field on martensite variant distribution is negligible compared to the distribution arising from strain compensation during transformation.

#### IV. SUMMARY

Measurements of fundamental thermodynamic and kinetic properties of  $\text{Ni}_{54}\text{Fe}_{19}\text{Ga}_{27}$  single crystals showed that the structural transition occurs as very sharp anomalies in resis-

tivity, specific heat, and magnetization. The amplitude and narrowness of the anomaly at the structural phase transition in  $\text{Ni}_{54}\text{Fe}_{19}\text{Ga}_{27}$  suggest an avalanche like character of martensitic transformation. The jump of resistivity at transition to martensite phase and lower value of density of states in martensite as compared to austenite supports the hypothesis of a Jahn-Teller nature of structural phase transition.

Temperature dependent magnetization measurements show the same transformation sequence as in active Ni-Mn-Ga compounds during cooling: Paramagnetic austenite/Ferromagnetic austenite/Ferromagnetic martensite. Additionally, these measurements suggest that ferrimagnetic order exists in this nonstoichiometric compound.

The saturation magnetizations in martensite and austenite phases differ in the vicinity of structural transformation by about 10%. This can be ascribed to the different Curie temperatures of the phases. In spite of the difference of saturation magnetization of the phases, the effect of magnetic field on transformation is insignificant. Notable magnetocrystalline anisotropy has been measured in the martensitic phase. This is much smaller compared to Ni-Mn-Ga compounds. No characteristic jump of magnetization marking the variant reorientation has been observed in this sample. These circumstances limit the potential use of this specific compound as magnetically driven shape-memory alloy.

These conclusions should be tested in a broader composition range since Heusler alloys have two free parameters to vary composition and thereby transition temperatures and intrinsic properties.

#### ACKNOWLEDGMENTS

This work was supported by RFBR Grant No. 07-02-91580, Ministry of Science and Education of Russian Federation 2007-3-1.3-11-04-154 and by DFG through SPP 1239.<sup>27</sup>

<sup>1</sup>A. N. Vasil'ev, V. D. Buchel'nikov, T. Takagi, V. V. Khovailo, and E. I. Estrin, *Phys. Usp.* **46**, 559 (2003).

<sup>2</sup>K. Ullakko, J. K. Huang, C. Kanter, V. V. Kokorin, and R. C. O'Handley, *Appl. Phys. Lett.* **69**, 1966 (1996).

<sup>3</sup>R. C. O'Handley, *J. Appl. Phys.* **83**, 3263 (1998).

<sup>4</sup>O. Heczko, A. Sozinov, and K. Ullakko, *IEEE Trans. Magn.* **36**, 3266 (2000).

<sup>5</sup>A. Vasil'ev and T. Takagi, *Int. J. Appl. Electromagn. Mech.* **20**, 37 (2004).

<sup>6</sup>V. V. Khovailo, V. Novosad, T. Takagi, D. A. Filippov, R. Z. Levitin, and A. N. Vasil'ev, *Phys. Rev. B* **70**, 174413 (2004).

<sup>7</sup>O. Söderberg, A. Sozinov, Y. Ge, S.-P. Hannula, and V. K. Lindroos, in *Handbook of Magnetic Materials*, edited by J. Buschow (Elsevier Science, Amsterdam, 2006), Vol. 16, pp. 1–39.

<sup>8</sup>R. D. James and M. Wuttig, *Philos. Mag. A* **77**, 1273 (1998).

<sup>9</sup>T. Kakeshita, T. Tekeuchi, T. Fukuda, T. Saburi, R. Oshima, S. Muto, and K. Kishio, *Mater. Trans., JIM* **41**, 882 (2000).

<sup>10</sup>A. N. Vasil'ev, A. D. Bozhko, V. V. Khovailo, I. E. Dikstein, V. G. Shavrov, V. D. Buchelnikov, M. Matsumoto, S. Suzuki, T.

Takagi, and J. Tani, *Phys. Rev. B* **59**, 1113 (1999).

<sup>11</sup>A. Fujita, K. Fukamichi, F. Gejima, R. Kainuma, and K. Ishida, *Appl. Phys. Lett.* **77**, 3054 (2000).

<sup>12</sup>M. Wuttig, J. Li, and C. Craciunescu, *Scr. Mater.* **44**, 2393 (2001).

<sup>13</sup>K. Oikawa, T. Ota, T. Ohmori, Y. Tanaka, H. Morito, A. Fujita, R. Kainuma, K. Fukamichi, and K. Ishida, *Appl. Phys. Lett.* **81**, 5201 (2002).

<sup>14</sup>Z. H. Liu, H. Liu, X. X. Zhang, M. Zhang, X. F. Dai, H. N. Hu, J. L. Chen, and G. H. Wu, *Phys. Lett. A* **329**, 214 (2004).

<sup>15</sup>R. F. Hamilton, C. Efstathiou, H. Sehitoglu, and Y. Chumlyakov, *Scr. Mater.* **54**, 465 (2006).

<sup>16</sup>Z. H. Liu, H. N. Hu, G. D. Liu, Y. T. Cui, M. Zhang, J. L. Chen, G. H. Wu, and G. Xiao, *Phys. Rev. B* **69**, 134415 (2004).

<sup>17</sup>P. J. Brown, A. P. Gandy, K. Ishida, R. Kainuma, T. Kanomata, H. Morito, K.-U. Neumann, K. Oikawa, and K. R. A. Ziebeck, *J. Phys.: Condens. Matter* **19**, 016201 (2007).

<sup>18</sup>D. Varshney and N. Kaurav, *Eur. Phys. J. B* **37**, 301 (2004).

<sup>19</sup>S. Chikazumi, *Physics of Ferromagnetism* (Clarendon, Oxford,

- 1997), p. 144.
- <sup>20</sup>H. Zijlstra, *Experimental Methods in Magnetism* (North-Holland, Amsterdam, 1967), p. 129.
- <sup>21</sup>A. Aharoni, *Introduction to the Theory of Ferromagnetism* (Clarendon, Oxford, 1996), Chap. 4.
- <sup>22</sup>M. D. Kuz'min, Phys. Rev. Lett. **94**, 107204 (2005) [and also M. D. Kuz'min, M. Richter, A. N. Yaresko, Phys. Rev. B **73**, 100401(R) (2006)].
- <sup>23</sup>H. Morito, A. Fujita, K. Fukamichi, R. Kainuma, K. Ishida, and K. Oikawa, Appl. Phys. Lett. **83**, 4993 (2003).
- <sup>24</sup>P. J. Webster, K. R. A. Ziebeck, S. L. Town, and M. S. Peak, Philos. Mag. B **49**, 295 (1984).
- <sup>25</sup>J. Enkovaara, O. Heczko, A. Ayuela, and R. M. Nieminen, Phys. Rev. B **67**, 212405 (2003).
- <sup>26</sup>L. Straka and O. Heczko, J. Appl. Phys. **93**, 8636 (2003).
- <sup>27</sup>[www.magneticshape.de](http://www.magneticshape.de).